Performance of Multiuser MIMO-OFDM System with Fractional Sampling in Street Canyon Area

Kenta Eguchi, Mamiko Inamori, Yukitoshi Sanada
Dept. of Electronics and Electrical Engineering, Keio University, Yokohama, Japan
Email:eguchi@snd.elec.keio.ac.jp, {inamori, sanada}@elec.keio.ac.jp

***Abstract*—This paper presents performance of a multiuser MIMO-OFDM (MU-MIMO) system with Fractional Sampling (FS) on a street canyon model. The MU-MIMO system has been investigated to improve the channel capacity in cellular systems. However the capacity of the MU-MIMO is deteriorated in an urban environment such as a street canyon due to a high correlation between antennas. Through FS it is possible to separate multipath components and realize diversity. FS works effectively when the correlation between the users are high. Numerical results through computer simulation shows that the capacity improves with the FS by about 3.5 bps/Hz.**

I. Introduction

High-speed, large-capacity, and highly reliable communications can be realized with recent advances in digital processing technologies. Orthogonal Frequency Division Multiplexing (OFDM) has been widely investigated and developed as a modulation scheme that meets the recent demands on wireless communications. OFDM achieves high frequency utilization efficiency by the use of orthogonal subcarriers [1], [2]. These days, OFDM is employed, for example, in wireless LAN and WiMAX standards, and many other broadband wireless systems [3], [4], [5].

A Multiple-Input Multiple-Output (MIMO) technique has been investigated for the OFDM system to realize high-speed and reliable transmission [6]. The MIMO technique employs multiple antennas both at the transmitter and the receiver. In the future, a multiuser MIMO (MU-MIMO) system is expected to support multiple users accessing one base station (BS) to improve the total capacity on cellular systems [7], [8], [9]. However, in an urban environment such as a street canyon area, where the cellular systems are employed, the propagation of the signal suffers from a keyhole effect and the MIMO capacity decreases due to a high correlation between the signals received by the different users or different antennas of the same user [10], [11].

On the other hand, a fractional sampling (FS) scheme in the OFDM system has been proposed [12]. Through the FS, it is possible to separate multipath components and obtain diversity gain. Moreover, further diversity gain can be realized by selecting the sampling points [13]. With this scheme, the correlation among the antennas is expected to decrease because the channel response of each sampling point is independent.

In this paper, the channel capacity of the MU-MIMO-OFDM system with the FS in the street canyon area under the condition of the high correlation among the antennas is evaluated. In the proposed system, the FS reduces the correlation between the signals received by the different users or the different antennas. The precoding for null forming in the MU-MIMO system then works effectively while the power of the signal reaches the receiver efficiently.

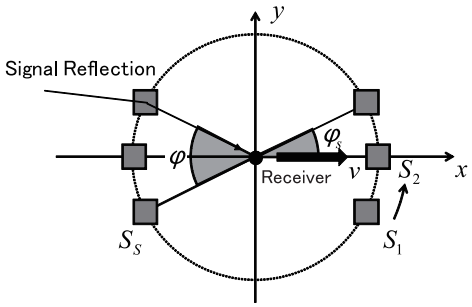

Fig. 1. Street canyon model.

This paper is organized as follows. Section II explains the street canyon model and the MU-MIMO-OFDM with the FS as the proposed scheme. The numerical results through computer simulation are shown in Section III. Finally, conclusions are presented in Section IV.

II. System Model

A. Street Canyon Model

The assumed channel model is shown in Fig. 1. The street canyon channel is generated by Jakes' fading model with the narrower arrival angles of the signals [14], [15]. As shown in Fig. 1, the arrival angles are limited from the front $(0^\circ \pm \frac{\phi}{2})$ and the back $(180^\circ \pm \frac{\phi}{2})$ of the cove. The fading waveform experienced at the position of (x, y) is expressed as

$$T(t,x,y) = \frac{1}{\sqrt{S}} \sum_{s=1}^{S} \exp[j(2\pi f_D t \cos\phi_s) + \rho_s] \cdot \exp[j2\pi(x\cos\phi_s + y\sin\phi_s)], \quad (1)$$

where f_D is the maximum Doppler frequency, S is the number of the incident signals, and ϕ_s is the arrival angle of the sth incident signal.

In Fig. 1, the correlations among the received signals at the positions of $(t, 0, 0)$, $(t, 0, d)$, $(t, \delta, 0)$ are shown in Figs. 2 and 3. In Fig. 2, two receivers are located on the y axis and the correlation decreases little by little as the antenna elements are separated. If the two receivers are placed on the x axis, the correlation oscillates in every half wavelength.

978-1-4673-1881-5/12/$31.00 ©2012 IEEE

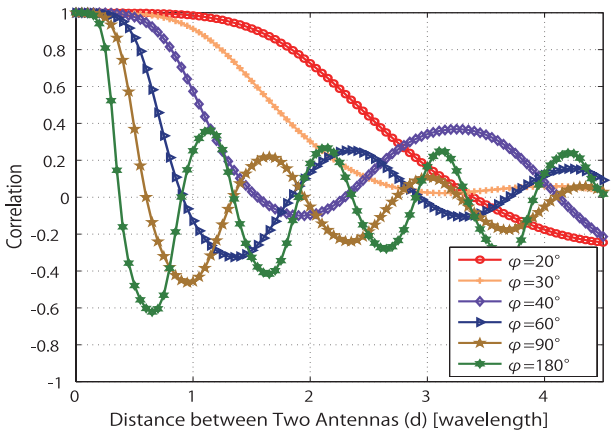

Fig. 2. Correlation between $T(t,0,0)$ and $T(t,0,d)$.

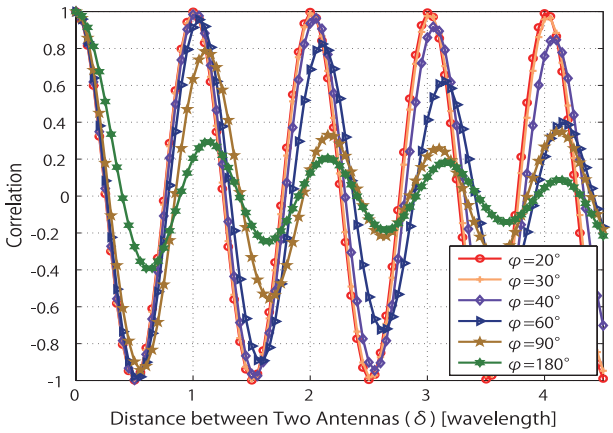

Fig. 3. Correlation between $T(t,0,0)$ and $T(t,\delta,0)$.

B. FS-Multiuser MIMO-OFDM

1) Multiuser MIMO-OFDM: The block diagram of a MU-MIMO-OFDM system is shown in Fig. 4. It is assumed that the BS has M_t $(1,...m_t,...,M_t)$ transmit antennas. The total number of the user terminals supported by the BS simultaneously is K and the kth user terminal has M_r^k $(1,...m_r,...,M_r^k)$ receive antennas. Suppose an information symbol on the lth subcarrier for the kth user is $s_{m_t}^k[l]$ $(l=0,...,N-1)$, the OFDM symbol in time domain is then given as

$$\begin{aligned} u_{m_t}^k[n] &= \frac{1}{\sqrt{N}}\sum_{l=0}^{N-1} T_{m_t}^k[l]s_{m_t}^k[l]e^{j\frac{2\pi nl}{N}}, \\ n &= 0,...,N-1, \end{aligned} \tag{2}$$

where n $(n=0,1,...,N-1)$ is the time index on the lth subcarrier and $T_{m_t}^k[l]$ is the precoding coefficient of the m_tth transmit antenna for the kth user. A guard interval (GI) with the length of N_{GI} is appended before transmission. The length of one OFDM symbol is $P := N + N_{GI}$.

The baseband signal at the output of the filter is given

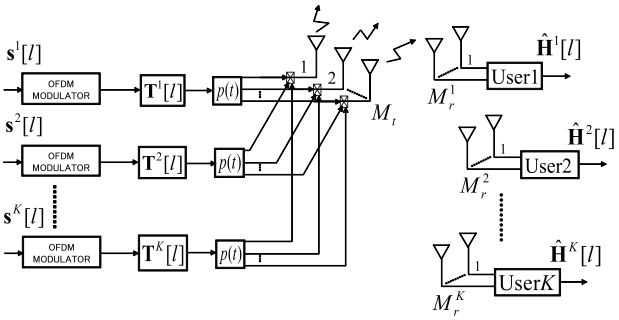

Fig. 4. Multiuser MIMO-OFDM.

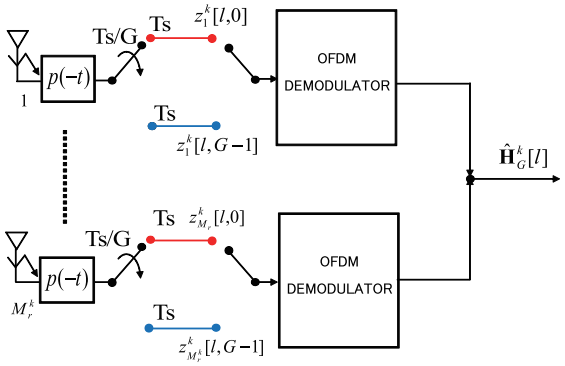

Fig. 5. Receiver model with FS.

by $x_{m_r,m_t}^k(t) = \sum_{n=0}^{P-1} u_{m_t}^k[n]p(t-nT_s)$ where $p(t)$ is the impulse response of the baseband filter and T_s is the symbol duration. This signal is upconverted and transmitted through a multipath channel to the m_rth antenna of the kth user with an impulse response, $c_{m_r,m_t}^k(t)$. The received signal after downconversion is given as

$$y_{m_r}^k(t) = \sum_{n=0}^{P-1} u_{m_t}^k[n]h_{m_r,m_t}^k(t-nT_s) + v_{m_r}(t). \tag{3}$$

Here, $h_{m_r,m_t}^k(t)$ is the impulse response of the composite channel between the m_tth transmit antenna of the BS and the m_rth receive antenna of the kth terminal. It is given by $h_{m_r,m_t}^k(t) := p(t) \star c_{m_r,m_t}^k(t) \star p(-t)$, where $\star$ denotes convolution, and $v_{m_r}^k(t)$ is the additive Gaussian noise filtered at the kth receiver. On the multipath channel, $h_{m_r,m_t}^k(t)$ can be expressed in a baseband form as

$$h_{m_r,m_t}^k(t) = \sum_{i=0}^{N_{m_r,m_t}^k-1} \alpha_{m_r,m_t,i}^k p_2(t-\tau_i^k) \tag{4}$$

where $p_2(t) := p(t) \star p(-t)$ is the deterministic correlation of $p(t)$. It is assumed that the channel in Eq. (4) has N_{m_r,m_t}^k path components, $\alpha_{m_r,m_t,i}^k$ and $\tau_{m_r,m_t,i}^k$ are the amplitude and the delay of the ith path between the m_tth transmit antenna and the m_rth receive antenna of the kth user, respectively.

2) User Model with FS: The block diagram of the kth user terminal in the MU-MIMO-OFDM with the FS is shown

in Fig. 5. The FS is implemented and the received signal is sampled at the rate of T_s/G. The polyphase components of the sampled signal can be expressed as

$$\begin{aligned} y^k_{m_r}[n, g^k_{m_r}] &= \sum_{q=0}^{P-1} u^k_{m_t}[q] h^k_{m_r,m_t}[n-q, g^k_{m_r}] \\ &\quad + v^k_{m_r}[n, g^k_{m_r}], \\ g^k_{m_r} &= 0, ..., G-1, \end{aligned} \tag{5}$$

where $g^k_{m_r}$ is the sampling index for the m_rth antenna of the kth user. One of the sampling index, $g^k_{m_r}$, is selected on each antenna as shown in Fig. 5. The received signal, the channel response, and the noise component for the $g^k_{m_r}$th sampling point are given as

$$y^k_{m_r}[n, g^k_{m_r}] := y^k_{m_r}(nT_s + g^k_{m_r} T_s/G), \tag{6}$$

$$h^k_{m_r,m_t}[n, g^k_{m_r}] := h^k_{m_r,m_t}(nT_s + g^k_{m_r} T_s/G), \tag{7}$$

$$v^k_{m_r}[n, g^k_{m_r}] := v^k_{m_r}(nT_s + g^k_{m_r} T_s/G). \tag{8}$$

After removing the GI and taking DFT on each subcarrier, the received symbol is given by

$$z^k_{m_r}[l, g^k_{m_r}] = H^k_{m_r,m_t}[l, g^k_{m_r}] s^k_{m_t}[l] + w^k_{m_r}[l, g^k_{m_r}] \tag{9}$$

where $z^k_{m_r}[l, g^k_{m_r}]$, $H^k_{m_r,m_t}[l, g^k_{m_r}]$, and $w^k_{m_r}[l, g^k_{m_r}]$ are similarly given as

$$z^k_{m_r}[l, g^k_{m_r}] = \sum_{n=0}^{N-1} y^k_{m_r}[n, g^k_{m_r}] e^{-j\frac{2\pi ln}{N}}, \tag{10}$$

$$H^k_{m_r,m_t}[l, g^k_{m_r}] = \sum_{n=0}^{N-1} h^k_{m_r,m_t}[n, g^k_{m_r}] e^{-j\frac{2\pi ln}{N}}, \tag{11}$$

$$w^k_{m_r}[l, g^k_{m_r}] = \sum_{n=0}^{N-1} v^k_{m_r}[n, g^k_{m_r}] e^{-j\frac{2\pi ln}{N}}. \tag{12}$$

Therefore, the received signals on the lth subcarrier for M^k_r antennas with the FS are written as

$$\begin{aligned} \mathbf{z}^k_G[l] &= \mathbf{H}^k_G[l] \sum_{i=1}^{K} \mathbf{T}^i_G[l] \mathbf{s}^i[l] + \mathbf{w}^k_G[l], \\ l &= 0, ..., N-1, \end{aligned} \tag{13}$$

where $\mathbf{z}^k_G[l]$, $\mathbf{H}^k_G[l]$, and $\mathbf{w}^k_G[l]$ are the received signal matrix, the channel response matrix, and the Gaussian noise matrix for the FS receiver and are given as

$$\mathbf{z}^k_G[l] = \begin{bmatrix} z^k_{1,1}[l, g^k_1] & \cdots & z^k_{1,M_t}[l, g^k_1] \\ \vdots & \ddots & \vdots \\ z^k_{M^k_r,1}[l, g^k_{M^k_r}] & \cdots & z^k_{M^k_r,M_t}[l, g^k_{M^k_r}] \end{bmatrix}, \tag{14}$$

$$\mathbf{H}^k_G[l] = \begin{bmatrix} H^k_{1,1}[l, g^k_1] & \cdots & H^k_{1,M_t}[l, g^k_1] \\ \vdots & \ddots & \vdots \\ H^k_{M^k_r,1}[l, g^k_{M^k_r}] & \cdots & H^k_{M^k_r,M_t}[l, g^k_{M^k_r}] \end{bmatrix}, \tag{15}$$

$$\mathbf{w}^k_G[l] = \begin{bmatrix} w^k_{1,1}[l, g^k_1] & \cdots & w^k_{1,M_t}[l, g^k_1] \\ \vdots & \ddots & \vdots \\ w^k_{M^k_r,1}[l, g^k_{M^k_r}] & \cdots & w^k_{M^k_r,M_t}[l, g^k_{M^k_r}] \end{bmatrix}, \tag{16}$$

and $\mathbf{T}^k_G[l] = [T^k_{1,G}[l], T^k_{2,G}[l], ..., T^k_{M_t,G}[l]]^T$ is then calculated from the following equation,

$$\begin{bmatrix} \mathbf{H}^1_G[l] \\ \vdots \\ \mathbf{H}^{k-1}_G[l] \\ \mathbf{H}^{k+1}_G[l] \\ \vdots \\ \mathbf{H}^K_G[l] \end{bmatrix} \mathbf{T}^k_G[l] = 0. \tag{17}$$

It can be written as $\mathbf{T}^k_G[l] = \mathbf{V}^k_G[l] \mathbf{A}^k_G[l]$ where $\mathbf{A}^k_G[l]$ is regarded as the $n_k \times L_k$ transmit processing matrix [16]. n_k is then expressed as

$$n_k = M_t - \sum_{i=1, i\neq k}^{K} M^i_r, \quad M_t > \sum_{i=1, i\neq k}^{K} M^i_r \tag{18}$$

and L_k is the number of data streams to the kth user terminal. $\mathbf{V}^k_G[l]$ is obtained from channel's singular value decomposition (SVD) by

$$\begin{aligned} &\begin{bmatrix} \mathbf{H}^1_G[l] \\ \vdots \\ \mathbf{H}^{k-1}_G[l] \\ \mathbf{H}^{k+1}_G[l] \\ \vdots \\ \mathbf{H}^K_G[l] \end{bmatrix} \\ &= \begin{bmatrix} \tilde{\mathbf{U}}^k_G[l] & \mathbf{U}^k_G[l] \end{bmatrix} \cdot \begin{bmatrix} \Sigma & 0 \\ 0 & 0 \end{bmatrix} \cdot \begin{bmatrix} \tilde{\mathbf{V}}^k_G[l]^{\mathbf{H}} \\ \mathbf{V}^k_G[l]^{\mathbf{H}} \end{bmatrix}. \end{aligned} \tag{19}$$

3) Channel Capacity: If the transmitter knows the CSI, the capacity of the kth user terminal with a water-filling algorithm can be written as

$$C(\mathbf{H}^k_p[l], \frac{P_T}{K}) = \sum_{i=1}^{r} \log_2(1 + \frac{P_T \gamma^k_i}{K M_t} \lambda^k_i) \tag{20}$$

where P_T is the total energy of the transmit signal, and r is the rank of the precoded channel matrix $\mathbf{H}^k_p[l] = \mathbf{H}^k_G[l] \mathbf{V}^k_G[l]$, λ^k_i $(i = 1, 2, ...r)$ is the positive eigenvalues of $\mathbf{H}^k_p[l] \mathbf{H}^k_p[l]^H$, and γ^k_i satisfies $\gamma^k_i = \left(\mu - \frac{M_t}{P_T \lambda^k_i}\right)^+$ ($(x)^+ = 0$ if $x \leq 0$, $(x)^+ = x$ if $x > 0$) while $\sum_{i=1}^{r} \gamma^k_i = M_t$ is given by the water-filling algorithm [17]. Therefore, the total capacity of the FS-MU-MIMO-OFDM system under the condition of equal power allocation among the users at the transmitter is obtained by

$$C_{total} = \frac{1}{N} \sum_{l=1}^{N} \sum_{k=1}^{K} C(\mathbf{H}^k_p[l], \frac{P_T}{K}). \tag{21}$$

4) Sampling Point Selection on Each Receive Antenna: In the FS-MU-MIMO-OFDM system, a sampling point on each antenna can be selected based on the CSI. Therefore, the system achieves path diversity on each antenna using the

TABLE I
SIMULATION CONDITIONS.

Modulation scheme	OFDM
No. of packets	10000
No. of subcarriers	64
No. of data subcarriers	48
No. of transmit antennas M_t	4
No. of user terminals K	2
No. of receive antennas on each user M_r^k	2
FS order G	1, 2
E_s/N_0 [dB]	0, 10, 20
Channel model	2 path street canyon 2 path i.i.d. Rayleigh
Channel information	Ideal
Velocity of users v [m/sec]	10
Arrival angle ϕ [$^\circ$]	20
Correlation between the users R_δ	0.99($\delta = 4.02$ wavelength) 0.15($\delta = 4.25$ wavelength)
Correlation between the receive antennas R_d	0.99($d = 0.2$ wavelength) 0.15($d = 3.2$ wavelength)

FS. On the other hand, if G is set to 1, it is equivalent to the conventional MU-MIMO-OFDM.

In the receiver, the set of the sampling points with the best channel response among the $G^{\Sigma_{k=1}^K M_r^k}$ combinations is selected. The correlation between the antenna elements on the same or different users can be reduced by the selection of the sampling points, and the capacity of the system increases.

III. NUMERICAL RESULTS

A. Simulation Conditions

The channel capacity of the FS-MU-MIMO-OFDM is evaluated through computer simulation. Simulation conditions are shown in Table I. The size of DFT/IDFT is set to 64. The number of data subcarriers and pilot subcarriers are 48 and 4. The composite impulse response $p(t) \star p(-t)$ is assumed to be a truncated sinc pulse with the duration of $2T_s$ [12]. The number of the transmit antennas at the BS is 4, the number of the user terminals is 2, and each user has 2 receive antennas. The FS order is $G = 1, 2$. As the channel models, a 2 path street canyon model and a 2 path i.i.d. Rayleigh fading model are assumed for comparison. The delay of the paths is set to $T_s/2$ [18]. In the street canyon model, the velocity of the users is 10 m/sec and the arrivals angle of the signals are within ± 10 ($\phi = 20$) degrees. The 2 user terminals are located on the x axis with the distance of δ and the 2 antennas of each user terminal are separated in the direction of the y axis with the distance of d in Fig. 1. The distance between the users (δ) is 4.02 wavelength (high correlation between the users, coefficient of correlation $R_\delta = 0.99$) or 4.25 wavelength (low correlation, $R_\delta = 0.15$). The distance between the antennas of the same user (d) is 0.2 wavelength (high correlation between the antennas on the same user, coefficient of correlation $R_d = 0.99$) or 3.2 wavelength (low correlation, $R_d = 0.15$).

B. Numerical Results

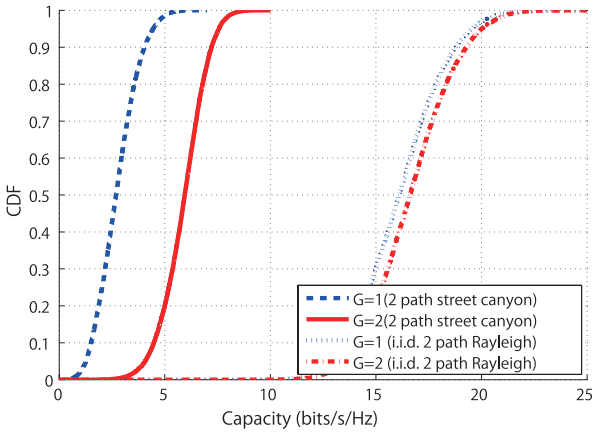

Fig. 6. CDF of channel capacity (2 path street canyon, $R_\delta = 0.99, R_d = 0.99$).

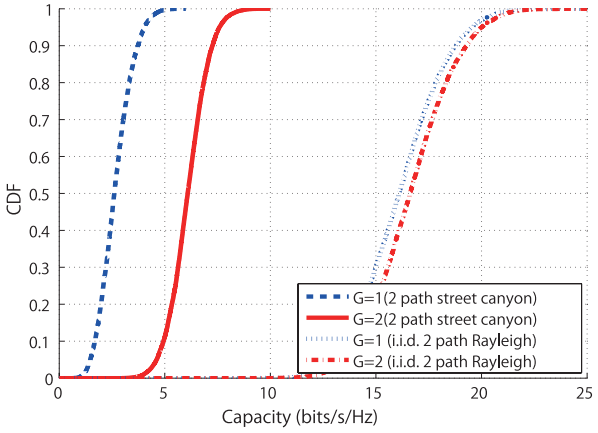

Fig. 7. CDF of channel capacity (2 path street canyon, $R_\delta = 0.99, R_d = 0.15$).

1) Channel Capacity: The cumulative distribution functions (CDFs) of the channel capacity on the 2 path street canyon with the FS-MU-MIMO-OFDM are compared with those on the independent 2 path Rayleigh channel in Figs. 6-8. E_s/N_0 is set to 20dB. In Figs. 6 and 7, R_δ is high. The capacity on the street canyon channel with the conventional scheme ($G = 1$) decreases to 2.5 bps/Hz at CDF=0.5. Through the FS ($G = 2$), the capacity improves up to 6.0 bps/Hz. In Fig. 8, the capacity on the street canyon channel with $G = 1$ decreases to 12.5 bps/Hz at CDF=0.5 and it improves with $G = 2$ up to 13.5 bps/Hz. Comparing Figs. 7 and 8, the degradation of the capacity caused by high correlation between the users R_δ is large. However, the degradation of the capacity caused by high correlation between the antennas R_d is a little. This is because the null direction of the antennas is formed to the desired user with the precoding for the high user correlation case while the water-filling algorithm works effectively with the low correlation users.

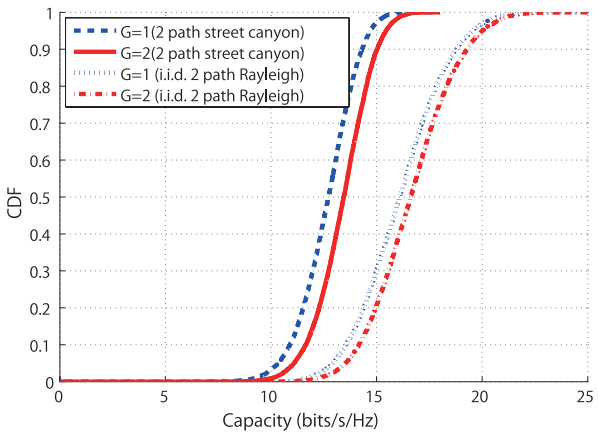

Fig. 8. CDF of channel capacity (2 path street canyon, $R_\delta = 0.15, R_d = 0.99$).

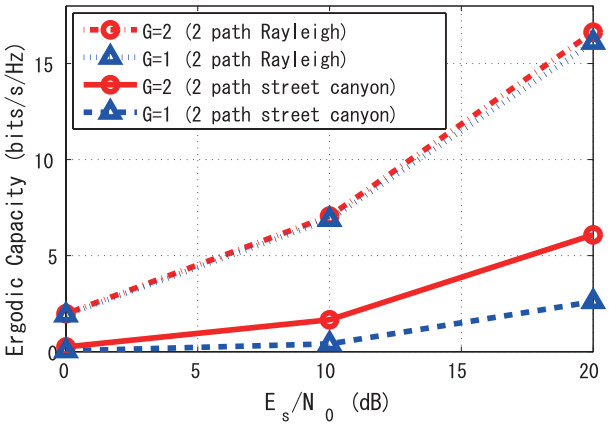

Fig. 9. Ergodic capacity v.s. E_s/N_0 (2 path street canyon, $R_\delta = 0.99, R_d = 0.15$).

2) Ergodic Capcaity v.s. E_s/N_0: The ergodic capacity v.s. E_s/N_0 on the 2 path street canyon model of the FS-MU-MIMO-OFDM is compared with that for the independent 2 path Rayleigh channel in Fig. 9. This figure shows that the FS $(G = 2)$ improves the capacity as compared to that with the conventional system $(G = 1)$ in all E_s/N_0 regions when the correlation between the antennas on the users is high. In addition, large improvement is observed in the high E_s/N_0 region. The same tendency can be observed for the low correlation user cases though the improvement is limited.

IV. Conclusions

In this paper, to improve the capacity of the MU-MIMO-OFDM system on the street canyon channel, the FS scheme is implemented in the receiver to realize path diversity. The FS scheme works effectively when the correlation between the users is high. This is because the precoding in the MU-MIMO forms the null to both of the users and the reduction of the correlation through path diversity improves the capacity effectively. It has been shown for the case of the high correlation between the users that the proposed scheme improves the capacity about 3.5 bps/Hz. On the other hand, for the case of the high correlation among the antennas of the same user, the water-filling algorithm compensates the capacity and the improvement with the FS is limited.

Acknowledgement

This work is supported in part by a Grant-in-Aid for the Global Center of Excellence for high-Level Global Cooperation for Leading-Edge Platform on Access Spaces and Grant-in-Aid for Scientific Research (C) under Grant No.22560390 from the Ministry of Education, Culture, Sport, Science, and Technology in Japan.

References

[1] S. Weinstein, "The History of Orthogonal Frequency Division Multiplexing," IEEE Trans. on Broadcasting, IEEE Communications Magazine, pp. 26-35, Nov. 2009.
[2] J. Wang, J. Song, Z-X. Yang, L. Yang, and J. Wang, "Frames Theoretic Analysis of Zero-Padding OFDM over Deep Fading Wireless Channels," IEEE Trans. on Broadcasting, vol. 52, no. 2, pp. 252-260, Jun. 2006.
[3] IEEE 802.11a-Part 11: Wireless LAN Medium Access Control(MAC) and Physical Layer(PHY) specifications; Highspeed Physical Layer in the 5GHz Band.
[4] IEEE 802.11g-Part 11: Wireless LAN Medium Access Control(MAC) and Physical Layer(PHY) specifications; Highspeed Physical Layer in the 2.4GHz Band.
[5] IEEE 802.16eTM-Part 16: Air Interface for Fixed and Mobile Broadband Wireless Access Systems.
[6] H. Bölcskei, D. Gesbert, and A.J.Paulraj, "On the Capacity of OFDM-Based Spatial Multiplexing Systems," IEEE Trans. on Communications, vol. 50, no. 2, pp. 225-234, Feb. 2002.
[7] Q. H. Spencer, A. L. Swindlehurst and M. Haardt, "Zero-Forcing Methods for Downlink Spatial Multiplexing in MU-MIMO Channels," IEEE Trans. on Signal Processing, vol. 52, no. 2, Feb. 2004.
[8] K. -K. Wong, R. D. Murch, R. S.-K. Cheng, K. B. Letaief, "Optimizing the Spectral Efficiency of MU-MIMO Smart Antenna Systems," IEEE WCNC 2000, Sept. 2000.
[9] J.-H. Chang, L. Tassiulas, F. Rashid-Farrokhi, "Joint Transmitter Receiver Diversity for Efficient Space Division Multiaccess," IEEE Trans. on Wireless Communications, vol. 1, no. 1, pp. 16-27, Jan. 2002.
[10] A. -F. Molisch, "A Generic Model for MIMO Wireless Propagation Channels in Macro- and Microcells," IEEE Trans. on Signal Processing, vol. 52, no. 1, pp. 61-71, Jan. 2004.
[11] G. Levin, S. Loyka "On the Outage Capacity Distribution of Correlated Keyhole MIMO Channels," IEEE Trans. on Information Theory, vol. 54, no. 7, pp. 3232-3245, July 2008.
[12] C. Tepedelenlioğlu and R. Challagulla, "Low-Complexity Multipath Diversity Through Fractional Sampling in OFDM," IEEE Trans. on Signal Processing, vol. 52, no. 11, pp. 3104-3116, Nov. 2004.
[13] H. Nishimura, M. Inamori, Y. Sanada, and M. Ghavami, "Non-uniform Sampling Point Selection in OFDM Receiver with Fractional Sampling," IET Trans. on Communications, vol. 5, issue 4, pp. 554-562, April 2011.
[14] W. Jakes, Microwave Mobile Communications, NJ, IEEE Press, 1994.
[15] A. Kuchar, J.-P. Rossi, and E. Bonek, "Directional Macro-Cell Channel Characterization from Urban Measurements," IEEE Trans. on Antennas and Propagation, vol. 48, no. 2, Feb. 2000.
[16] L. Choi, R. D. Murch, "A Transmit Preprocessing Technique for Multiuser MIMO Systems Using a Decomposition Approach," IEEE Trans. on Wireless Communications, Vol. 3, No. 1, Jan. 2004.
[17] D. P. Palomar, R. Fonollosa, "Practical Algorithms for a Family of Waterfilling Solutions," IEEE Trans. on Signal Processing, vol. 53, no. 2, pp. 686-695, Feb. 2005.
[18] A. F. Molisch, "Effect of Far Scatterer Clusters in MIMO Outdoor Channel Models," IEEE Vehicular Technology Conference 2003, vol. 1 pp. 534-538, 2003.